Electromagnetic near-field codebook design for general antenna arrays

Miguel Rodrigo Castellanos
Dept. of Electrical Engineering and Computer Science
University of Tennessee, Knoxville, TN 37966
mrcastellanos@utk.edu

Robert W. Heath, Jr.
Dept. of Electrical and Computer Engineering
University of California San Diego, La Jolla, CA 92093
rwheathjr@ucsd.edu

***Abstract*—Precoding codebooks facilitate efficient channel state information acquisition in high-dimensional MIMO systems. Most codebook designs, however, are agnostic to the antenna array composition and the underlying gain pattern profiles. We leverage an electromagnetic characterization of the antenna array manifold to generalize the codebook design problem. Specifically, we formulate the codebook design problem in a manner that incorporates polarization, near-field propagation and the antenna array characteristics. Our proposed approach is also flexible enough to adapt to different antenna types and even to heterogenous arrays. Our numerical results demonstrate that the electromagnetic-based codebooks achieve higher beamforming gains than approaches that neglect antenna effects.**

I. Introduction

Despite similarities in communication objectives, wireless devices use a broad range of antennas. Present-day networks exhibit a high degree of heterogeneity at the physical layer. Systems can operate at a variety of vastly different frequency ranges, such as sub-6 GHz, upper mid-band, and millimeter-wave [1]. Though fundamentally similar, mobile devices, base stations and vehicles are often equipped with different types of antenna arrays that vary in dimension, physical size and element makeup. Some devices even contain various types of radios that operate simultaneously, and each of these can leverage a diferent antenna [2]. As wireless functionality becomes more ubiquitous, these design-level variations are leading to a highly diverse and heterogenous wireless ecosystem.

Beamforming codebooks are nearly ubiquitous in communication systems, and antenna characteristics can drastically affect codebook design. Antennas can vary in terms of their gain patterns, their polarization characteristics, and their frequency response, all of which influence the desirability of a particular beamforming codebook [3]. A directional antenna, for example, will exhibit a narrower beam pattern than an isotropic antenna if both arrays use weights from the same codebook. The polarization of an antenna also has a significant effect on the received signal power depending on the mismatch between the transmit and receive polarizations [4]. Overall antennas are an important component in determining the array pattern. Codebook design relies on optimizing beam patterns for a given channel distribution, but the stochastic channel behavior is highly dependent on the array.

Prior work has largely pursued antenna-agnostic codebook design or assumed that the antenna characteristics are incorporated into channel models. A variety of past studies assume particular array structures and antenna types to facilitate codebook design [5]–[7]. Antenna and array effects can also be modeled with stochastic models, and codebook design can be adapted to the ensuing channel distributions [8], [9]. In recent years, machine learning methods have also been leveraged for codebook design by incorporating the channel and array properties into learning models [10], [11]. A key disadvantage of all these approaches is the lack of analytical framework to understand the effect of the antennas on codebook design.

Physically-consistent array models are key in scenarios in which the antenna characteristics cannot be ignored. While hardware and antenna modeling for MIMO applications has been the subject of prior work, new advances in reconfigurability make the model more important. In a reconfigurable setting, the antenna model parameters can be optimized to increase performance in terms of achievable rate and beamforming gain [4], [12]. Densely packed arrays with high mutual coupling can be exploited to provide superdirective beams with large gain relative to their radiative power [13]. Future wireless arrays may even be composed of different antenna types interleaved with each other to enable wideband communication from low to high frequencies [1]. New applications and performance objectives for wireless make hardware modeling more important than ever.

We apply our EM-based array model in [14] for codebook design. The EM array manifold model incorporates all key properties of the antennas in the far-field and near-field and can be applied to arbitrary array geometries. Because of this, the proposed methods do not require any assumptions regarding the antenna type or the array structure. We use the EM manifold to formulate beam design metrics in terms of beamforming gain and beam efficiency. We then design beam codebooks under a transmit power constraint and a radiated power constraint. Numerical simulations showcase the advantages of the proposed codebook design for highly coupled arrays and conformal arrays.

Notation: A column vector is denoted as bold lowercase letter $\mathbf{a}$, and a matrix is denoted as a bold uppercase letter $\mathbf{A}$. The transpose of $\mathbf{A}$ is denoted as $\mathbf{A}^{\mathsf{T}}$, the conjugate of $\mathbf{A}$ is denoted as $\mathbf{A}^{\mathsf{c}}$, and the conjugate transpose of $\mathbf{A}$ is denoted as $\mathbf{A}^{*}$. The unit imaginary number is denoted as j.

II. System model and problem formulation

A. Signal model

We consider a communication system with an N antenna transmitter and a single antenna receiver. For simplicity, we assume a narrowband link at frequency f with perfect synchronization. The receiver is located at point $\mathbf{p} \in \mathbb{R}^3$. At discrete time ℓ, The transmitter beamforms the symbol $s[\ell] \in C$ with vector $\mathbf{w}[\ell] \in \mathbb{C}^N$. The transmit symbol $s[\ell]$ is zero-mean and unit-variance. Within the coherence time, the channel $\mathbf{h}(\mathbf{p}) \in \mathbb{C}^T$ from the transmitter to the receiver at $\mathbf{p}$ is constant. Letting $n[\ell]$ denote the additive Gaussian noise with variance σ^2, the receive signal is

$$y[\ell] = \mathbf{h}^*(\mathbf{p})\mathbf{w}[\ell]s[\ell] + n[\ell]. \tag{1}$$

We do not place any restriction on $\mathbf{p}$, meaning that the receiver may lie in the near-field or far-field of the transmitter.

We assume line-of-sight propagation between the transmitter and the receive antenna. We apply the framework in [14] to model the channel in terms of the transmit electromagnetic array manifold and the receive polarization. The receive electric field consists of three different components: a radial component, an azimuthal component, and an elevation component. We assume that $\mathbf{p}$ is sufficiently far from the array such that the radial component is negligible. The array manifold vectors for the two angular dimensions can be grouped into an $N \times 2$ matrix $\mathbf{A}(\mathbf{p})$ referred to as the EM manifold. The EM manifold incorporates the transmit polarization as well as the antenna gain patterns for any kind of antenna structure. We assume the receiver has polarization represented by the unit vector $\mathbf{b} \in \mathbb{C}^2$ that dictates the strength of the strength of the vertical and horizontal polarizations. Letting ρ denote a large-scale fading component, we model the channel as

$$\mathbf{h}(\mathbf{p}) = \sqrt{\rho}\mathbf{A}(\mathbf{p})\mathbf{b}. \tag{2}$$

Intuitively, $\mathbf{A}$ gives the transmit radiated field components that are then combined by the receive polarization $\mathbf{b}$. This model does not assume any particular array geometry or antenna type and therefore provides an extremely flexible framework.

B. Performance objectives and constraints

The transmitter aims to simultaneously maximize the receive signal power at the receiver while satisfying constraints on sidelobes and radiated power. We define the beamforming gain at a receiver with location $\mathbf{p}$ and polarization $\mathbf{b}$ for a given $\mathbf{w}$ as

$$G(\mathbf{w}, \mathbf{p}, \mathbf{b}) = \frac{\mathbf{w}^*\mathbf{A}(\mathbf{p})\mathbf{b}\mathbf{b}^*\mathbf{A}^*(\mathbf{p})\mathbf{w}}{\mathbf{w}^*\mathbf{w}}. \tag{3}$$

The beamforming gain characterizes the receive power but does not account for wasted power radiated in other directions. To address this issue we also consider the ratio of the main beam gain compared to the overall beam gain, which we call the beam efficiency. Let $\mathbf{p}$ have norm r and let S_r denote the spherical surface with radius r surrounding the transmitter. We define the beam efficiency as

$$\eta(\mathbf{w}, \mathbf{p}, \mathbf{b}) = \frac{G(\mathbf{w}, \mathbf{p}, \mathbf{b})}{\frac{1}{4\pi r^2}\int_{S_r} G(\mathbf{w}, \mathbf{p}', \mathbf{b}) d\mathbf{p}'}, \tag{4}$$

Using the definition from (3), η can be simplified as

$$\eta(\mathbf{w}, \mathbf{p}, \mathbf{b}) = \frac{\mathbf{w}^*\mathbf{A}(\mathbf{p})\mathbf{b}\mathbf{b}^*\mathbf{A}^*(\mathbf{p})\mathbf{w}}{\frac{1}{4\pi r^2}\int_{S_r} \mathbf{w}^*\mathbf{A}(\mathbf{p}')\mathbf{A}^*(\mathbf{p}')\mathbf{w}\, d\mathbf{p}'} \tag{5}$$

$$= \frac{\mathbf{w}^*\mathbf{A}(\mathbf{p})\mathbf{b}\mathbf{b}^*\mathbf{A}^*(\mathbf{p})\mathbf{w}}{\mathbf{w}^*\left\{\int_{S_r} \frac{1}{4\pi r^2}\mathbf{A}(\mathbf{p}')\mathbf{b}\mathbf{b}^*\mathbf{A}^*(\mathbf{p}')\, d\mathbf{p}'\right\}\mathbf{w}} \tag{6}$$

Defining $\mathbf{X_b} = \left\{\int_{S_r} \frac{1}{4\pi r^2}\mathbf{A}(\mathbf{p}')\mathbf{b}\mathbf{b}^*\mathbf{A}^*(\mathbf{p}')\, d\mathbf{p}'\right\}$, the beam efficiency can be expressed as the generalized Rayleigh quotient

$$\eta(\mathbf{w}, \mathbf{p}, \mathbf{b}) = \frac{\mathbf{w}^*\mathbf{A}(\mathbf{p})\mathbf{b}\mathbf{b}^*\mathbf{A}^*(\mathbf{p})\mathbf{w}}{\mathbf{w}^*\mathbf{X_b}\mathbf{w}}. \tag{7}$$

We denote $\mathbf{X_b}$ as the characteristic pattern matrix for the array since $\mathbf{w}^*\mathbf{X_b}\mathbf{w}$ gives the average array gain on the sphere S_r. We will use both the beamforming gain and the beam efficiency as codebook design metrics.

We assume the transmitter chooses $\mathbf{w}$ from a codebook of M beams $\mathcal{W} = \{\mathbf{w}_1, \mathbf{w}_2, \cdots, \mathbf{w}_M\}$. For a given channel, The transmitter cycles through the codebook and selects the beam with the highest gain. We denote the maximum gain at $\mathbf{p}$ over the codebook as

$$S(\mathcal{W}, \mathbf{p}, \mathbf{b}) = \max_{\mathbf{w}\in\mathcal{W}} G(\mathbf{w}, \mathbf{p}, \mathbf{b}). \tag{8}$$

Both the receive position and polarization are assumed to be unknown and random. We measure performance as

$$S_{\mathsf{ave}}(\mathcal{W}) = \mathbb{E}_{\mathbf{p},\mathbf{b}}\left[S(\mathcal{W}, \mathbf{p}, \mathbf{b})\right]. \tag{9}$$

This metric quantifies the average gain assuming the best beam is chosen for transmission.

To simplify the analysis, we make two key assumptions regarding $\mathbf{p}$ and $\mathbf{b}$. We assume that $\mathbf{p}$ follows a discrete uniform distribution over a finite set of points $\mathcal{P} = \{\mathbf{p}_1, \mathbf{p}_2, \cdots, \mathbf{p}_K\}$. We also assume that the receiver is linearly polarized with a uniformly distributed polarization angle φ. In other words, the receive polarization is $\mathbf{b}(\varphi) = [0, \cos\varphi, \sin\varphi]^\mathsf{T}$ with φ uniformly distributed over $[0, 2\pi)$. The codebook metric then simplifies as

$$S_{\mathsf{ave}}(\mathcal{W}) = \frac{1}{2\pi K}\int_0^{2\pi}\sum_{k=1}^{K} S(\mathcal{W}, \mathbf{p}_k, \mathbf{b}(\varphi))\, d\varphi. \tag{10}$$

In the following, we leverage the EM manifold to design beamforming codebooks.

III. Codebook design

We consider codebook design under two kinds of power constraints: a transmit power constraint and a radiated power constraint. We also simplify codebook design by setting $M = K$ and assuming that each beam in the codebook corresponds to a point $\mathbf{p}_k$.

A. Transmit power constraint

We first assume the only constraint imposed on the codebook is that each beam must satisfy $\|\mathbf{w}\|^2 \leq P$. The codebook optimization is

$$\mathcal{W}^\star = \underset{\mathcal{W}}{\operatorname{argmax}}\ S_{\mathsf{ave}}(\mathcal{W}) \tag{11}$$

$$s.t. \quad \mathbf{w}^*\mathbf{w} \leq P\ \forall \mathbf{w} \in \mathcal{W}. \tag{12}$$

From the assumption that each codewords corresponds to one point, each beam can be optimized individually as

$$\mathbf{w}_k^\star = \underset{\mathbf{w}^*\mathbf{w}\leq 1}{\operatorname{argmax}}\ \frac{1}{2\pi}\int_0^{2\pi} G(\mathbf{w}, \mathbf{p}_k, \mathbf{b}(\varphi))\, d\varphi. \tag{13}$$

Letting $\mathbf{A}_k = \mathbf{A}(\mathbf{p}_k)$ The objective can be written as

$$\begin{aligned}\frac{1}{2\pi}\int_0^{2\pi} G(\mathbf{w}, \mathbf{p}_k, \mathbf{b}(\varphi))\, d\varphi &= \frac{1}{2\pi}\int_0^{2\pi} \frac{\left\|\mathbf{b}^*\mathbf{A}^*(\mathbf{p})\mathbf{w}\right\|^2}{\|\mathbf{w}\|^2}\, d\varphi \\ &\frac{1}{2\pi}\int_0^{2\pi} \frac{\mathbf{w}^*\mathbf{A}_k\mathbf{b}\mathbf{b}^*\mathbf{A}_k^*\mathbf{w}}{\|\mathbf{w}\|^2}\, d\varphi \\ &= \frac{\mathbf{w}^*\mathbf{A}_k\mathbf{A}_k^*\mathbf{w}}{4\pi\|\mathbf{w}\|^2},\end{aligned} \tag{14}$$

where the last equality comes from the fact that $\int_0^{2\pi} \mathbf{b}\mathbf{b}^*\, d\varphi = 1/2\mathbf{I}$. From (14), the singular value decomposition (SVD) of $\mathbf{A}_k$ provides the solution to (13). Let $\mathbf{A}_k^*$ have SVD $\mathbf{A}_k^* = \mathbf{U}_k\mathbf{S}_k\mathbf{V}_k$. Then $\mathbf{w}_k^\star$ should be set to the dominant right singular vector $\mathbf{v}_{1,k}$ scaled by an arbitrary complex scalar α_k as

$$\mathbf{w}_k^\star = \alpha_k\sqrt{P}\mathbf{v}_{1,k}, \tag{15}$$

and the codebook is set to $\mathcal{W}^\star = \left\{\mathbf{w}_k^\star\right\}_{k=1}^K$.

Interestingly, the uniform distribution of linear receive polarizations results in a codebook that leverages the dominant array polarization. The SVD of the EM manifold reveals the inherent copolarization (CP) and cross-polarization (XP) of the array. The left singular matrix $\mathbf{U}_k = [\mathbf{u}_1\mathbf{u}_2]$ is a 2×2 matrix that yields an orthonormal polarization basis. From the definition of $G(\mathbf{w}, \mathbf{p}, \mathbf{b})$, the polarization $\mathbf{b}$ that results in the highest gain is the dominant left singular vector, i.e., $\mathbf{u}_1$. Likewise, the polarization resulting in the lowest gain is $\mathbf{u}_2$. The proposed codebook chooses the beam that would correspond to a receiver polarized as $\mathbf{b} = \mathbf{u}_1$.

B. Radiated power constraint

In many settings, wireless devices are limited in terms of radiated power to limit interference and EM exposure. This power constraint can be formulated in terms of the characteristic matrix $\mathbf{X}_\mathbf{b}$ as $\mathbf{w}^*\mathbf{X}_\mathbf{b}\mathbf{w}$. We consider an average power constraint in terms of user polarizations. Letting Q denote the radiated power constraint and defining $\mathbf{X} = \mathbb{E}_\mathbf{b}\left[X_\mathbf{b}\right]$, the constraint is

$$\mathbf{w}^*\mathbf{X}\mathbf{w} \leq Q. \tag{16}$$

The codebook optimization problem in this case is

$$\mathcal{W}^\star = \underset{\mathcal{W}}{\operatorname{argmax}}\ S_{\mathsf{ave}}(\mathcal{W}) \tag{17}$$

$$s.t. \quad \mathbf{w}^*\mathbf{X}\mathbf{w} \leq Q\ \forall \mathbf{w} \in \mathcal{W}. \tag{18}$$

As before, we optimize before the beams individually

$$\mathbf{w}_k^\star = \underset{\mathbf{w}^*\mathbf{X}\mathbf{w}\leq Q}{\operatorname{argmax}}\ \frac{1}{2\pi}\int_0^{2\pi} G(\mathbf{w}, \mathbf{p}_k, \mathbf{b}(\varphi))\, d\varphi. \tag{19}$$

Due to the radiated power constraint, an equivalent optimization can be formulated in terms of the beam efficiency as

$$\mathbf{w}_k^\star = \underset{\mathbf{w}^*\mathbf{X}\mathbf{w}=Q}{\operatorname{argmax}}\ \frac{1}{2\pi}\int_0^{2\pi} \eta(\mathbf{w}, \mathbf{p}_k, \mathbf{b}(\varphi))\, d\varphi \tag{20}$$

$$= \underset{\mathbf{w}^*\mathbf{X}\mathbf{w}=Q}{\operatorname{argmax}}\ \frac{\mathbf{w}^*\mathbf{A}_k\mathbf{A}_k^*\mathbf{w}}{4\pi\mathbf{w}^*\mathbf{X}\mathbf{w}} \tag{21}$$

Let $\mathbf{A}_k^*\mathbf{X}^{-1/2}$ have SVD $\mathbf{A}_k^*\mathbf{X}^{-1/2} = \mathbf{U}_k\mathbf{S}_k\mathbf{V}_k$. We obtain the optimal solution from the dominant right singular vector of $\mathbf{V}_k$ with the addition of a spatial correlation term

$$\mathbf{w}_k^\star = \alpha_k\sqrt{Q}\mathbf{X}^{1/2}\mathbf{v}_{1,k}. \tag{22}$$

The radiated power matrix is, in general, not equal to the identity matrix. The radiated power constraint leads to narrow beams with significantly decreased sidelobes. It is also important to note that the codebook design problem can also easily adapt to radiated power constraints over more constrained regions by simply changing how $\mathbf{X}$ is computed. For example, $\mathbf{X}$ can be computed over a small region in front of the array to model a user exposure constraint as discussed in [14].

IV. Numerical results

We evaluate the EM-based codebook designs with a few different antenna array types. We use the method in [14] to compute the EM manifold and compare the performance of the proposed codebooks with a codebook designed with the traditional isotropic manifold.

A. Array model

We briefly describe the array model in [14] and how to compute the EM manifold matrix. The main idea is to partition each antenna in the array into small sections, each of which can be modeled as a point source. The nth antenna in the array is partitioned into K_n pieces.

We let $\mathbf{m}_{n,k}^{(\ell)}$ denote the dipole moment induced in the kth segment of the nth antenna when the array is excited by a unit amplitude excitation. We also define $\mathbf{p}_{n,k}$ as the position vector from the center of the kth segment of the nth antenna to $\mathbf{p}$. The antenna moment vector for the nth antenna is given as

$$\overline{\mathbf{m}}_n^{(\ell)} = [(\mathbf{m}_{n,1}^{\ell})^\mathsf{T}, \cdots, (\mathbf{m}_{n,K_n}^{(\ell)})^\mathsf{T}]^\mathsf{T}, \tag{23}$$

and the array given vector is

$$\overline{\mathbf{m}}_{\mathsf{arr}}^{\ell} = [(\overline{\mathbf{m}}_1^{(\ell)})^\mathsf{T}, \cdots, (\overline{\mathbf{m}}_N^{(\ell)})^\mathsf{T}]^\mathsf{T}. \tag{24}$$

Letting the total number of segments be $\overline{K} = \sum_{n=1}^N K_n$, $\overline{\mathbf{m}}_{\mathsf{arr}}^{\ell}$ is a $3\overline{K}$ length vector because each $\mathbf{m}_{n,k}^{\ell}$ has three spatial components. We then define $\overline{\mathbf{M}} = [\overline{\mathbf{m}}_{\mathsf{arr}}^{(1)}, \cdots, \overline{\mathbf{m}}_{\mathsf{arr}}^{(N)}]$ as the $3\overline{K} \times N$ effective array moment matrix, which captures the current distribution over the entire array when each element is excited.

The electric field is obtained by summing the contributions of each point source. We define block matrices $\overline{\mathbf{R}}_{\mathsf{arr}}^{\mathsf{T}}(\mathbf{p})$ as the $3 \times \overline{K}$ array rotational coherence matrix, and $\overline{\mathbf{T}}_{\mathsf{arr}}(\mathbf{p})$ as the $3\overline{K} \times 3\overline{K}$ array dipole field transform. The expressions for both of these are described in more detail in [14]. The array electric field is obtained through the summation of the contributions from the extended dipole array as

$$\boldsymbol{\mathcal{E}}_{\mathsf{arr}}(\mathbf{p}, \mathbf{w}) = \overline{\mathbf{R}}_{\mathsf{arr}}^{\mathsf{T}}(\mathbf{p})\overline{\mathbf{T}}_{\mathsf{arr}}(\mathbf{p})\overline{\mathbf{M}}\mathbf{w}. \tag{25}$$

The $N \times 3$ EM manifold matrix is then defined as

$$\mathbf{A}^{*}(\mathbf{p}) = \overline{\mathbf{R}}_{\mathsf{arr}}^{\mathsf{T}}\overline{\mathbf{T}}_{\mathsf{arr}}(\mathbf{p})\overline{\mathbf{M}}. \tag{26}$$

We note that $\overline{\mathbf{M}}$ must be obtained from electromagnetic simulations on the array but that it does not depend on the position $\mathbf{p}$. This characterization differs from prior work in which simulations are used to obtain the electric field at each point of interest. Our approach only requires the current distribution of the array, and the rest of the model can be obtained in closed-form.

B. Codebook performance

We leverage electromagnetic simulations to measure the codebook performance. The gain of the array is measured relative to a single half-wavelength dipole located at the origin. We use a half-wavelength dipole rather than an ideal isotropic antenna because the former is polarized and has near-field effects. We denote $\boldsymbol{\mathcal{E}}_{\mathsf{ref}}(\mathbf{p})$ as the electric field radiated by a the reference half-wavelength dipole antenna, and let $\boldsymbol{\mathcal{E}}_{\mathsf{sim}}(\mathbf{p}, \mathbf{w})$ be the simulated electric field at $\mathbf{p}$ when the array is excited by $\mathbf{w}$. We define the array gain referenced to a dipole as

$$G_{\mathsf{arr}}(\mathbf{p}, \mathbf{w}, \mathbf{b}) = \frac{\left|\mathbf{b}^{\mathsf{T}}\boldsymbol{\mathcal{E}}_{\mathsf{sim}}(\mathbf{p}, \mathbf{w})\right|^2}{\left|\mathbf{b}^{\mathsf{T}}\boldsymbol{\mathcal{E}}_{\mathsf{ref}}(\mathbf{p})\right|^2}. \tag{27}$$

The numerical gain values are obtained from electromagnetic simulations using the MATLAB Antenna Toolbox.

We compare the performance of the proposed codebook under a transmit power constraint to that designed with the isotropic array manifold and the embedded array manifold. We let $\mathbf{c}_n$ denote the center of the nth antenna. The near-field isotropic manifold is given by

$$\mathbf{a}_{\mathsf{iso}}(\mathbf{p}) = \left[e^{-\mathrm{j}\beta\|\mathbf{p}-\mathbf{c}_0\|}, \ldots, e^{-\mathrm{j}\beta\|\mathbf{p}-\mathbf{c}_{N-1}\|}\right]^{\mathsf{T}}. \tag{28}$$

The isotropic manifold does not account for the polarization or the gain pattern of the antennas. The embedded array manifold is composed of the individual gain patterns from each antenna while in the presence of the other array elements. Because of this, the embedded manifold accounts for mutual coupling. Let $\mathbf{g}_n(\mathbf{p})$ denote the 2×1 embedded pattern vector for the horizontal and vertical polarizations, including both the gain and phase pattern for each polarization, observed at $\mathbf{p}$ from the nth antenna. The embedded manifold is then

$$\mathbf{A}_{\mathsf{emb}}(\mathbf{p}) = \left[\mathbf{g}_0^{\mathsf{T}}(\mathbf{p}), \ldots, \mathbf{g}_N^{\mathsf{T}}(\mathbf{p})\right]^{\mathsf{T}}. \tag{29}$$

The patterns in the embedded manifold are obtained from electromagnetic simulations that serve as the ground truth.

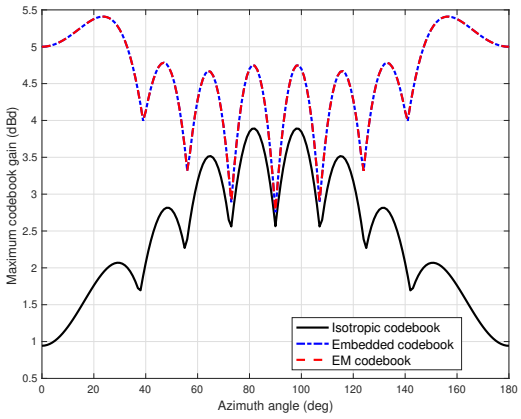

(a)

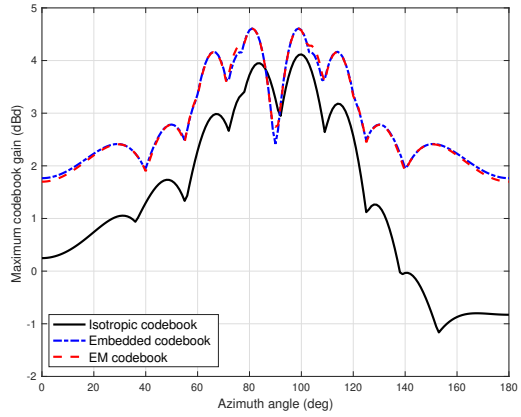

(b)

Fig. 1. Maximum beamforming gain over 8 codewords that uniformly cover an angular range of 180° for an (a) 8-element half-wave dipole array at quarter-wavelength spacing and (b) a 4-element conformal array with both half-wave dipoles and V-dipoles spaced at half-wavelength. The isotropic manifold assumes all antennas are identical and thus results in codebooks with lower gains. The proposed EM codebook performs as well as the upper bound obtained from an embedded gain pattern codebook.

Codebooks derived from the isotropic and embedded manifolds therefore serve as lower and upper bounds for the proposed method.

In the first simulation, we compare the codebook performance under a transmit power constraint with two kinds of arrays. The isotropic codebook is composed of matched-filter beams $\mathbf{w}_{k,\mathsf{iso}}^{\star} = \sqrt{P}\mathbf{a}_{\mathsf{iso}}(\mathbf{p}_k)/\left\|\mathbf{a}_{\mathsf{iso}}(\mathbf{p}_k)\right\|$. The codewords resulting from the embedded manifold are obtained from the SVD. Letting $\mathbf{v}_{1,k}$ be the dominant right singular vector of $\mathbf{A}_{\mathsf{emb}}(\mathbf{p}_k)$. The codewords are then set to $\mathbf{w}_{k,\mathsf{emb}}^{\star} = \sqrt{P}\mathbf{v}_{1,k}$. In Fig. 1, we show the maximum codebook gain averaged over linear user polarizations. The codebooks are designed to uniformly cover an angular range of 180° in the far-field with 8 beams. In Fig. 1(a), we show the codebook performance for an 8-element array of half-wave dipoles at quarter-wavelength spacing. Due to high mutual coupling, the isotropic manifold serves as a poor approximation of the array behavior, and the

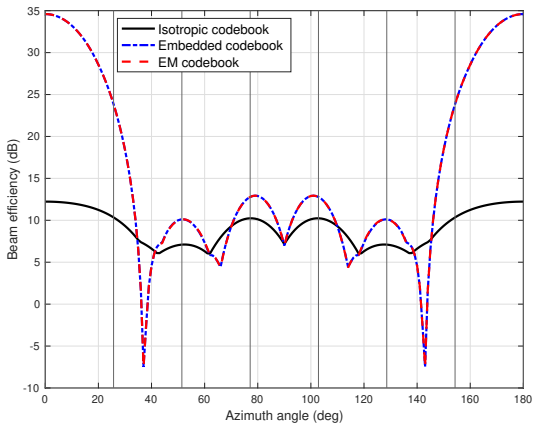

Fig. 2. Codebook beam efficiency, which is the ratio of the received power to the radiated power, of the isotropic, embedded, and proposed EM codebook. The proposed codebook shows a higher efficiency at the codebook directions by jointly maximizing beam gain while reducing radiated power.

EM codebook achieves higher gain across the angular range. The results also show that the EM codebook performs as well as the embedded codebook. The primary advantage of the EM manifold over the embedded codebook is flexibility. A new set of gain pattern measurements would be required to form a codebook for different $\mathbf{p}_k$. In contrast, the EM manifold can easily be leveraged to design new codebooks once $\overline{\mathbf{M}}$ is obtained from simulations.

In Fig. 1(b), we show how the EM manifold can also be leveraged in cases of a conformal array. We consider an array composed both V-dipoles and half-wave dipoles. Letting V denote a V-dipole and I denote a half-wave dipole, the array consists of 4 elements arranged as VIIV. The presence of multiple antenna types within the array deteriorates the performance of the isotropic codebook since it assumes all antennas are identical. The EM manifold demonstrates both the ability to design codebooks for diverse arrays and higher performance than the isotropic manifold.

We also compare the performance of the three codebooks under a radiated power constraint. We assume the same directions for codebook design as in the previous simulation. We measure the beam efficiency using EM simulations as

$$\eta_{\mathsf{arr}}(\mathbf{p},\mathbf{w},\mathbf{b}) = \frac{\left|\mathbf{b}^{\mathsf{T}}\boldsymbol{\mathcal{E}}_{\mathsf{sim}}(\mathbf{p},\mathbf{w})\right|^2}{\frac{1}{4\pi^2}\int_{S_r}\left|\mathbf{b}^{\mathsf{T}}\boldsymbol{\mathcal{E}}_{\mathsf{sim}}(\mathbf{p})\right|^2 dS_r}. \tag{30}$$

We assume that the isotropic manifold codebook ignores the radiated power constraint. The embedded manifold codebook is designed similarly to the EM codebook but uses the embedded manifold to calculate $\mathbf{X}$. We show the beam efficiency of the isotropic, embedded, and EM codebooks for an 8-element half-wave dipole array spaced at quarter-wavelength in Fig. 2. The proposed codebook demonstrates a higher efficiency at the codebook directions.

V. Conclusion

We have leveraged EM array modeling to formulate a codebook design optimization that accounts for polarization and mutual coupling. In the case that the receiver is linearly polarized, the proposed codebook aligns beams with the dominant array polarization. We also demonstrate how EM modeling can also be exploited to formulate a radiated power constraint on the codebook design problem. The proposed codebook significantly outperforms codebooks derived using the isotropic manifold in settings with high mutual coupling, diverse arrays, and radiated power constraints.

VI. Acknowledgements

This material is based upon work supported by the National Science Foundation under grants NSF-ECCS-2435261 and NSF-CCF-2435254, and the Army Research Office under grant W911NF2410107.

References

[1] S. Kang, M. Mezzavilla, S. Rangan, A. Madanayake, S. B. Venkatakrishnan, G. Hellbourg, M. Ghosh, H. Rahmani, and A. Dhananjay, "Cellular wireless networks in the upper mid-band," *IEEE Open J. Commun. Soc.*, vol. 5, pp. 2058–2075, 2024.

[2] W. Hong, "Solving the 5G mobile antenna puzzle: Assessing future directions for the 5G mobile antenna paradigm shift," *IEEE Microw. Mag.*, vol. 18, no. 7, pp. 86–102, Nov 2017.

[3] J. Mo, B. L. Ng, S. Chang, P. Huang, M. N. Kulkarni, A. Alammouri, J. C. Zhang, J. Lee, and W.-J. Choi, "Beam codebook design for 5G mmWave terminals," *IEEE Access*, vol. 7, pp. 98 387–98 404, 2019.

[4] M. R. Castellanos and R. W. Heath, "Linear polarization optimization for wideband MIMO systems with reconfigurable arrays," *IEEE Trans. Wireless Commun.*, vol. 23, no. 3, pp. 2282–2295, Nov. 2024.

[5] J. Zhang, Y. Huang, Q. Shi, J. Wang, and L. Yang, "Codebook design for beam alignment in millimeter wave communication systems," *IEEE Trans. Commun.*, vol. 65, no. 11, pp. 4980–4995, Nov. 2017.

[6] J. Song, J. Choi, and D. J. Love, "Common codebook millimeter wave beam design: Designing beams for both sounding and communication with uniform planar arrays," *IEEE Trans. Commun.*, vol. 65, no. 4, pp. 1859–1872, Feb. 2017.

[7] J. Chen, F. Gao, M. Jian, and W. Yuan, "Hierarchical codebook design for near-field mmwave MIMO communications systems," *IEEE Wireless Commun. Lett.*, vol. 12, no. 11, pp. 1926–1930, Jul. 2023.

[8] V. Raghavan, R. W. Heath, and A. M. Sayeed, "Systematic codebook designs for quantized beamforming in correlated MIMO channels," *IEEE J. Sel. Areas Commun.*, vol. 25, no. 7, pp. 1298–1310, Sep. 2007.

[9] D. Ying, F. W. Vook, T. A. Thomas, D. J. Love, and A. Ghosh, "Kronecker product correlation model and limited feedback codebook design in a 3D channel model," in *Proc. IEEE Int. Conf. Commun. (ICC)*, Sydney, NSW, Australia, Jun. 2014, pp. 5865–5870.

[10] R. M. Dreifuerst and R. W. Heath, "Machine learning codebook design for initial access and CSI type-II feedback in sub-6-GHz 5G NR," *IEEE Transactions on Wireless Communications*, vol. 23, no. 6, pp. 6411–6424, Jun. 2024.

[11] Y. Zhang, M. Alrabeiah, and A. Alkhateeb, "Reinforcement learning of beam codebooks in millimeter wave and terahertz MIMO systems," *IEEE Trans. Commun.*, vol. 70, no. 2, pp. 904–919, Feb. 2022.

[12] J. Carlson, M. R. Castellanos, and R. W. Heath, "Hierarchical codebook design with dynamic metasurface antennas for energy-efficient arrays," *IEEE Trans. Wireless Commun.*, vol. 23, no. 10, pp. 14 790–14 804, Oct. 2024.

[13] M. T. Ivrlač and J. A. Nossek, "Toward a circuit theory of communication," *IEEE Trans. Circuits Syst. I*, vol. 57, no. 7, pp. 1663–1683, Jul. 2010.

[14] M. R. Castellanos and R. W. Heath, "Electromagnetic manifold characterization of antenna arrays," *IEEE Trans. Wireless Commun.*, pp. 1–14, 2024.